Distributed Amorphous Ramp Construction in Unstructured Environments

Nils Napp and Radhika Nagpal

Abstract We present a model of construction using iterative amorphous depositions and give a distributed algorithm to reliably build ramps in unstructured environments. The relatively simple local strategy for interacting with irregularly shaped, partially built structures gives rise robust adaptive global properties. We illustrate the algorithm in both the single robot and multi-robot case via simulation and describe how to solve key technical challenges to implementing this abstract algorithm via a robotic prototype.

1 Introduction

Robots are best suited for dirty, dull, and dangerous tasks. This paper focuses on algorithms for the dirty and dangerous task of construction in unstructured terrain. Applications range from rapid disaster response, like building levees and support structures, to remote construction in mines or space. The requirement of working in unstructured terrain frequently coincides with a lack of sensing and computing infrastructure that enables coordination of multiple robots and deliberative planing, such as reliable global positioning and a consistent shared global state. Distributed algorithms that use limited local information and coordinate through stigmergy solve this problem as well as providing scalability. Robustness to poor sensing and irregular terrain can further be improved by using *amorphous* construction materials that comply to irregular obstacles. Such construction is locally reactive, both on the algorithmic level, i.e. where robots deposit based on local cues, and a

Nils Napp (nnapp@wyss.harvard.edu), Radhika Nagpal (rad@eecs.harvard.edu)
Harvard University
33 Oxford St
Cambridge MA 02138, USA
This work was supported by the Wyss Institute for Bioinspired Engineering

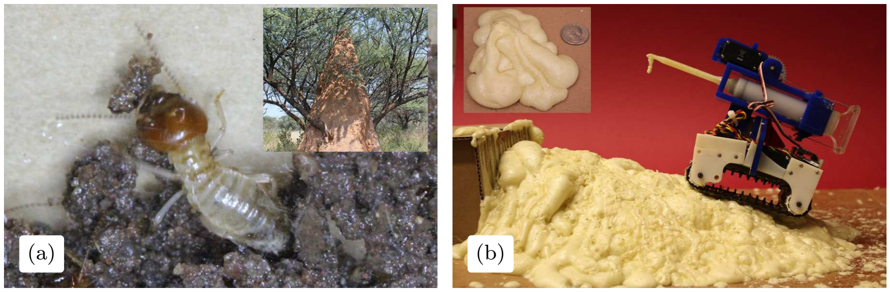

Fig. 1 Examples of amorphous construction. (a) Amorphous construction in biology. A termite preparing an amorphous dollop of mud for deposition. Inset shows a mound built around a tree. (b) Prototype of a construction robot. The robot was remote controlled to build a ramp using amorphous foam depositions. Inset shows a cone-shaped deposition.

physical level, i.e. amorphous construction materials react by changing shape to conform to their environment.

Our approach is inspired by biological systems, such as mound building termites [16], that are adept at reliably building in unstructured terrain, Fig. 1(a). Their skill combines robust scalable coordination through stigmergy and the use of amorphous building materials that interface with an irregular environment. We would like to endow scalable robot teams with similar skill, however an algorithmic foundation for doing so is lacking. Current models for autonomous robotic construction focus on assembling pre-fabricated building materials and cannot accommodate the continuous nature of amorphous building materials. The contribution of this paper is twofold:(A) A mathematical framework for describing and reasoning about robots that construct with amorphous materials, and (B) a distributed, locally reactive algorithm for adaptive ramp building in unstructured environments. This work is a step away from robots assembling discrete pre-fabricated components and instead embracing the messy continuous world, Fig. 1(b).

Section 2 presents mathematical models for amorphous construction and adaptive ramp building. Section 3 gives a local strategy for creating structures that robots can climb; Sec. 4 extends those results to include physical constraints for single and multiple robots. Section 5 discusses future work.

1.1 Related Work

Currently, there is much interest in the topic of robotic construction with mobile robots [3, 5, 4, 9, 13], as well as decentralized algorithms by which multiple robots can coordinate construction [1, 8, 11, 18, 15]. These systems are mainly focused on building pre-specified structures using lattice-based building materials. Lattice-based building blocks have good structural properties—being strong, stiff, and light—but place assumptions on the initial environment being well structured and devoid of obstacles. These methods are difficult to extend to unstructured environments with irregularly shaped obstacles. Furthermore, alignment and attachment restrictions affect all other aspects of design, for example adding complex assembly order constraints.

In contrast, amorphous building materials—e.g. foam, mud, sandbags or compliant blocks—sidestep these limitations. They can help compensate for uncertainty and measurement errors without requiring complex sensing or reasoning. For example, compliant and amorphous materials are used for rapidly building flood protection in disaster zones [6, 17] or pouring foundations over irregular terrain. Similarly, the requirement of fixed attachment orientations can be relaxed by using adhesive in the autonomous robotic construction of curved walls [2, 3]. The closely related work in [14] uses amorphous foam to rapidly adapt robot parts to a unknown tasks instead of adapting structures to unknown terrain. Digital manufacturing via CAD/CAM, and some large-scale robotic construction systems, such as [7], also use amorphous materials to build continuous shapes. While these systems are not specifically focused on construction in unstructured environments, we can exploit the materials and design principles to design robots that utilize amorphous materials.

2 Problem Formulation and Questions

We present a solution to the *adaptive ramp building* problem as a particular example of a distributed construction task in unstructured terrain. The problem is to design a deposition and motion strategy that allows robots starting from an arbitrary position to reach a goal, despite irregularly shaped obstacles. Robots can sense the goal direction, move on partially built structures, and deposit amorphous materials to make non-climbable structures climbable. The adaptive ramp building example shows how amorphous, noisy (see Sec. 4.1) construction materials can be used to create robust behavior and also provides a useful primitive behavior for solving more complex tasks. The remainder of this section presents a mathematical model for continuous structures, amorphous depositions, and climbable structures.

2.1 Mathematical Model for Continuous Structures

We model construction in two or three dimensions. The main theorems (Thm. 4–Thm. 6) and Alg. 1 work in both cases. Gravity constrains robots to move on one or two dimensional surfaces on which they can incrementally deposit construction material. Formally, we assume that the *construction area* Q is a connected, compact, and finite subset of $\mathbb{R}^1$ (or $\mathbb{R}^2$) and the domain

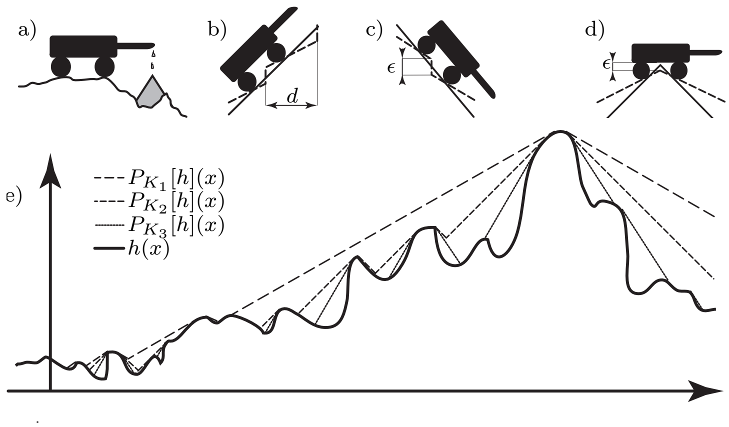

Fig. 2 Parameter Geometry. (a) Robot making an amorphous deposition. (b,c) Relation of K to the maximal steepness a robot can climb and descend, (solid) without discontinuity (dashed) with discontinuity. (d) Relation of steepness K to the required ground clearance to drive over the apex of a cone. (e) A height function on $h \in \mathcal{Q}^+$ and its projections onto Lipschitz functions with different parameters $K_3 > K_2 > K_1$.

of a bounded, non-negative height function $h : Q \to \mathbb{R}^+$. The graph of h, $(x, h(x))$ $x \in Q$, describes a *structure*. Robots move on structures and modify them.

If structures are modeled as functions, depositions are operators on functions. To distinguish the two, function spaces are denoted by scripted letters. For example, let $\mathcal{Q}$ be the space of real-valued, bounded functions on Q, and $\mathcal{Q}^+ \subset \mathcal{Q}$ the subset of non-negative ones. Function application to points is denoted by parentheses $(\cdot)$ and operator application to functions by brackets $[\cdot]$. For example, applying function $h \in \mathcal{Q}^+$ to a point $x \in Q$ is written as $h(x)$, and applying an operator $D : \mathcal{Q}^+ \to \mathcal{Q}^+$ to h is denoted by $D[h]$. In the case of functions, all relational symbols should be interpreted pointwise, e.g. given $h, g \in \mathcal{Q}^+$, $h \leq g \equiv h(x) \leq g(x)\ \forall x \in Q$.

One limitation of modeling both structures and deposition as functions is that many physical structures are not functions, i.e. they have overhangs. However, the benefit of this restrictive model is that it comes with analysis tools, such as continuity and integration, that are used to prove correctness of construction algorithms.

2.2 Model for Amorphous Deposition

We assume that robots can deposit amorphous construction material and control the volume and position, Fig. 1(b). The free surface of an amorphous deposition is modeled as a parameterized *shape function* $f \in \mathcal{Q}$. The bottom of each deposition conforms to the structure, Fig. 2(a). As a simple, yet sufficiently general, model each deposition is treated as a cone with its apex located at position (ϕ, σ) and steepness K_D, where $\phi \in Q$ and $K_D, \sigma \in \mathbb{R}^+$,

$$f_{(\phi,\sigma)}(x) = \sigma - K_D|\phi - x|. \tag{1}$$

The deposition operator D models interactions of depositions with the environment, here simply covering it. Given a structure $h \in \mathcal{Q}^+$ with $h(\phi) < \sigma$, the new structure after deposition $f_{(\phi,\sigma)}$ is given by $D : \mathcal{Q} \times \mathcal{Q}^+ \to \mathcal{Q}^+$, defined pointwise as

$$D[f_{(\phi,\sigma)}, h](x) = \max_{x \in Q}(f(x), h(x)). \tag{2}$$

Given an initial structure $h_0 \in \mathcal{Q}^+$ a structure is built by a sequence of depositions characterized by their shape parameters $(\phi_1, \sigma_1), (\phi_2, \sigma_2), (\phi_3, \sigma_3), \ldots$. The height function h_n after n depositions is defined recursively by

$$h_n(x) = D[f_{(\phi_n,\sigma_n)}, h_{n-1}](x). \tag{3}$$

After the n-th deposition, the local reactive rules of an individual robot direct it to move on h_n and to possibly make a deposition resulting in a new structure h_{n+1}.

This deposition model preserves continuity, independent of the particular parameter choices (ϕ_n, σ_n). In this and the following proofs, let $B_\epsilon(x)$ denote the *open ball* of radius ϵ around x, i.e. $y \in B_\epsilon(x)$ if and only if $|y - x| < \epsilon$.

Lemma 1 *Given a continuous $h_0 \in \mathcal{Q}^+$, h_n created according to (3), and $\epsilon \in \mathbb{R}^+$ then $\exists \delta$ s.t. $\forall x \in Q$ and $\forall y \in B_\delta(x) \subset Q$, $h_n(y) \in B_\epsilon(h_n(x))) \subset \mathbb{R}$.*

Proof. By continuity of h_0 and compactness of Q, for any given $\epsilon \in \mathbb{R}$ $\exists \delta'$ s.t. $\forall y \in B_\delta(x)$, $h_0(y) \in B_\epsilon(h(x))$. By construction of h_n, $\delta = \min\{\delta', \epsilon/K_D\}$ has the above property.

Our proposed solution to the ramp building problem can accommodate uncertainty in both the deposition location and size, see Sec. 4.1. However, to streamline the presentation we assume this exact deposition model in the following proofs.

2.3 Navigable Structures

Building a ramp means turning a structure that robots cannot climb into one they can climb. As such, any algorithm to adaptively build ramps needs a tractable description of climbable structures. This section defines the notion of *navigable* functions on Q, which represent climbable physical structures.

We use three parameters to describe robot specific motion constraints: $K \in \mathbb{R}^+$, which models the maximum steepness that a robot can drive up or down, $\epsilon \in \mathbb{R}^+$, which models the largest discontinuity (i.e. step up/down) a robot can freely move past, and $d \in \mathbb{R}^+$, which limits the concentration of discontinuities in a small area (i.e. robot length), Fig. 2(b)–2(d). Formally, navigable structures are locally (parameter d) close (parameter ϵ) to $K-$Lipschitz continuous [12, p. 594], i.e

$$|h(x) - h(y)| \leq K|x - y| \ \forall x, y \in Q, \tag{4}$$

with a constant $K \in \mathbb{R}^+$. Specifically, a function $h \in \mathcal{Q}$ is called navigable if and only if

$$|h(x) - h(y)| \leq \epsilon + K|x - y| \ \forall x, y \in Q \text{ and } |x - y| \leq d. \tag{5}$$

To reason about global guarantees of our local algorithms, we construct the operator P_K, defined by (7). It maps any structure to the *closest* K-Lipschitz function that can be built by only adding material, Fig. 2(e). At a given point $x \in Q$, P_K takes the maximum value of any cones that need to be added so all other points fulfill condition (4). There are two important properties of P_K. Firstly, by construction

$$P_K[h](x) \geq h(x) \ \forall h \in \mathcal{Q}. \tag{6}$$

Since we model depositions as additive, it is important $P_K[h]$ can be reached by only adding to h. Secondly, $P_K[h]$ returns the smallest function in $\mathcal{L}_K$, the space of K-Lipschitz functions on Q, in the following sense.

Theorem 2 *Given any two functions $h \in \mathcal{Q}$ and $g \in \mathcal{L}_K$ with $g \geq h$, the operator*

$$P_K[h](x) = \max_{y \in Q}\{h(y) - K|y - x|\} \tag{7}$$

with $K \in \mathbb{R}^+$, has the following properties:

1. $P_K[h]$ is K-Lipschitz,
2. $g \geq P_K[h]$.

The proof is given in Sec. 6.

The following theorem shows that if steeper features are allowed, less material needs to be added, Fig. 2(d).

Theorem 3 *Given an arbitrary function $h \in \mathcal{Q}$ and $K_1, K_2 \in \mathbb{R}^+$ with $K_1 \leq K_2$ the projections onto $\mathcal{L}_{K_1}$ and $\mathcal{L}_{K_2}$ follow $P_{K_2}[h] \leq P_{K_1}[h]$.*

Proof. For a given point $y \in Q$ in (7), $h(y) - K_2|y - x| \leq h(y) - K_1|y - x|$ since the $|y - x|$ is non-negative. □

Given an initial function h_0, the next section gives a locally reactive deposition strategy such that after N depositions h_N fulfills (5), i.e. is navigable, and bounded above by the closest dominating K-Lipschitz function, i.e. $h_n \leq P_K[h_0]$.

Algorithm 1 Local Deposition Strategy. Pick point pairs that imply a local non-navigable feature and deposit on the lower one.

Given $h \in \mathcal{Q}^+$.
$h_0 \leftarrow h$
while $\exists\, x, y \in Q$ s.t. $|x-y| \leq d,\ K|y-x| + \epsilon < |h_n(y) - h_n(x)|$ **do**
    if $h_n(x) < h_n(y)$ **then**
        $x' \leftarrow x$
        $y' \leftarrow y$
    else
        $x' \leftarrow y$
        $y' \leftarrow x$
    end if
    Pick any $\omega \in [\epsilon, h_n(y') - h_n(x') - K|x' - y'|]$
    Deposit at x' with height ω, i.e. $h_{n+1} = D[f_{(x', \omega + h_n(x'))}, h_n]$
end while

3 Local Reactive Deposition Algorithm

In a *local* deposition strategy, robots with limited sensing range $r \in \mathbb{R}^+$ (with $r > d$) move on top of the structure and *react* to features in their sensing range. The following algorithm relates local checks and depositions to global properties. The approach in Alg. 1 is to check for points that imply a non-navigable structure and deposit in such as way as to decrease the distance from the current structure to closest K-Lipschitz function $P_K[h_0]$. Specifically, Alg.1 searches for points $|y-x| \leq d$ s.t.

$$|y - x|K + \epsilon < |h(y) - h(x)|. \tag{8}$$

3.1 Correctness of Local Deposition Strategy

The correct behavior of Alg. 1 is that after a finite number of depositions the resulting structure h_N is navigable. The proof proceeds in two steps. (A) Thm. 4 shows progress, i.e. every deposition has a strictly positive volume. (B) Thm. 5 shows depositions obey the invariant upper bound $P_K[h_0]$. By combining them, Thm. 6 shows correct behavior, i.e. depositions according to Alg. 1 will stop once the structure is sufficiently close to $P_K[h_0]$. Note that since $P_K[h_0]$ is the smallest dominating K-Lipschitz function, Alg. 1 is efficient in the sense that it avoids unnecessary depositions, i.e. unnecessary to construct the conservatively navigable function $P_K[h_0]$.

The *volume* of a the difference between two structures $g, h \in \mathcal{Q}^+$ is given by

$$V(g, h) = ||g - h||_1 \equiv \int_Q |g(x) - h(x)|\ dx. \tag{9}$$

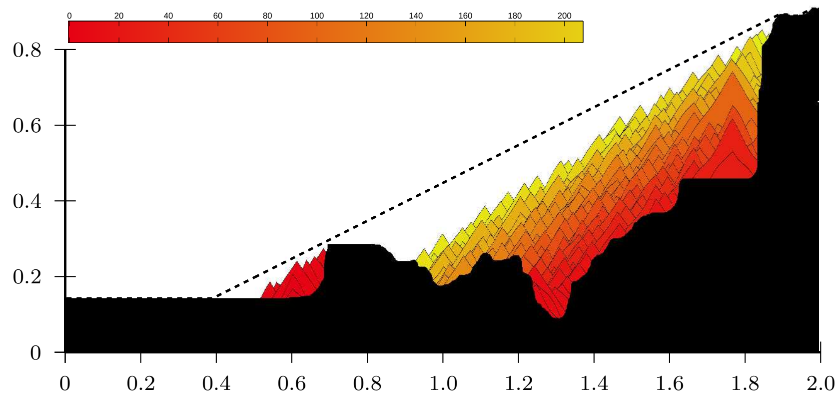

Fig. 3 Simulation of Alg. 2. Algorithm 2 is a special case of Alg. 1 that picks deposition sizes and positions. The initial structure h_0 is solid black. The upper bound $P_K[h_0]$ is shown as a dashed black line. The simulation parameters are: $Q = [0, 2]$, $K = 0.5$, $K_D = 1.5$, $\epsilon = 0.05$, and $d = 0.2$. Depositions progressively change color, see color-bar. The layered structure results from a robot starting at $x_0 = 0.2$ and trying to reach the goal position $x_* = 1.9$. It encounters the cliff on the right and during construction information is propagated backward through stigmergy, i.e. robot backing up to make new necessary depositions. As discussed in Sec. 4.1, the simulation also incorporates additive noise to the deposition shape function.

Similarly, for the given family of deposition functions the volume of a deposition is given by $V(D[f_{(\phi,\sigma)}, h], h)$.

Theorem 4 (Progress) *Given a pair of points $x, y \in Q$ s.t. $h_n(x) < h_n(y)$ and the property that*

$$|x - y|K + \epsilon < |h_n(x) - h_n(y)|,$$

depositing on x with a deposition of height

$$\omega \in [\epsilon, \frac{h_n(y) - h_n(x)}{K|x - y|}]$$

results in a volume $V(D[f_{(x,\omega)}, h_n], h_n) > \varepsilon$ that is bounded below by a strictly positive number ε.

Proof. Note that the deposition height is at least ϵ. By Lem. 1 there exists some δ s.t. h_n maps every $B_\delta(x) \subset Q$ into $B_{\epsilon/3}(h_n(x))$. As a result, $\forall p \in B_\delta(x)$, $h(p) < h(x) + \frac{\epsilon}{3}$ and $h(x) + \frac{2\epsilon}{3} < D[f_{(x,\omega)}, h_n](p)$. Therefore, $V(D[f_{(x,\omega)}, h_n], h_n) > \int_{B_\delta(x)} \frac{\epsilon}{3} = \varepsilon > 0$. □

Theorem 5 (Invariant) *Assuming that $K_D > K$, depositions made with Alg. 1 leave the mapping onto $\mathcal{L}_K$invariant, i.e. $P_K[h_n] = P_K[h_0]$.*

See Sec. 6 for proof.

Theorem 6 *Given an initial structure $h_0 \in \mathcal{Q}^+$, following Alg. 1 terminates after a finite number of steps, N; and for no points in Q does h_N fulfill condition (8), i.e. $\forall z \in Q$ and $x, y \in B_{\frac{d}{2}}(z)$,*

$$|x - y|K + \epsilon \geq |h_N(x) - h_N(y)|.$$

Proof. The expression for the remaining volume $V(P[h_0], h_n) = ||P[h_0] - h_n||_1 = \int_Q |P[h_0](x) - h_n(x)|dx$ can be rewritten as

$$\int_Q |P[h_0](x) - h_{n+1}(x) + h_{n+1}(x) - h_n(x)|dx.$$

By Thm. 5 and (6), $P[h_0](x) - h_{n+1}(x) \geq 0$ and $h_{n+1}(x) - h_n(x) \geq 0$, therefore

$$\begin{aligned} V(P[h_0], h_n) &= \int_Q |P[h_0](x) - h_{n+1}(x)|dx + \int_Q |h_{n+1}(x) - h_n(x)|dx \\ &= V(P[h_0], h_{n+1}) + V(h_{n+1}, h_n). \end{aligned}$$

By Thm. 4 the second term is bounded below by a positive number ε, thus

$$V(P[h_0], h_{n+1}) < V(P[h_0], h_n) - \varepsilon.$$

Since volume is always non-negative, condition (8) for making depositions must be violated after a finite number of steps N. □

4 Adaptive Ramp Building

The local deposition algorithm Alg. 1 does not specify which points to pick if the non-navigable condition (8) is true for multiple pairs, neither does it consider the physical extent of the robot or whether robots could reach deposition locations. The benefit of this vagueness is generality. Algorithm 1 works in arbitrary dimensions and an arbitrary number of robots making depositions in any order. It forms the theoretical underpinning for Alg. 2, Fig. 3, which takes such physical considerations into account, i.e. a local deposition and motion strategy that allows robot from an arbitrary starting position $x_0 \in Q$ to reach a goal $x_* \in Q$.

4.1 Adaptive Ramp Building with a Single Robot

To solve the adaptive ramp building problem, robots need to identify point pairs that imply a non-navigable feature and make depositions. Yet some

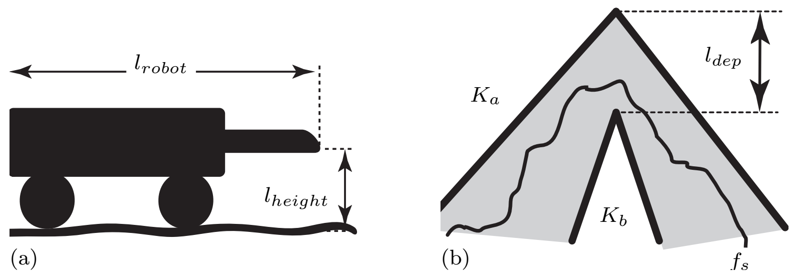

Fig. 4 Physical parameters. (a) Relevant robot dimension based on the prototype shown in Fig. 1(b). (b) Parameters for bounds of an arbitrary deposition shape function.

Algorithm 2 Adaptive ramp building. Given a structure h_0, an initial position x_0, and a goal position x_*, the following algorithm builds a ramp over irregular structures based on local sensing. Assume, w.l.o.g. that $x_0 < x_*$.

```
while x ≠ x_* do
    Move toward goal until ∃y ∈ [x, x + r] that the pair y and x + d violate condition
    (8) , or x = x_*
    if x ≠ x_* then
        Move to the lower the point. (Possible because all points in [x_0, x + r) are
        climbable).
        Pick height according to Alg.1 and condition (12).
        x ← x − 2d
    end if
end while
```

---

features are too large to be made navigable by a single deposition. In practice, robots might need to temporarily back away from the goal x_* to make previous depositions navigable.

Since deposition and motion constraints depend on the robot's physical dimensions, Fig. 4(a), additional parameter constraints are necessary to prove correctness of Alg. 2. First, to guarantee that robots have enough room to back up we assume they start at a point $x_0 \in Q$ on the initial structure h_0 and can move freely within a radius $r_0 \in \mathbb{R}^+$ without making any depositions,

$$P_K[h](x) = h(x), \quad \forall y \in B_{r_0}(x) \subset Q. \tag{10}$$

Second, key dimensions of the robot as well as the deposition parameter K_D need to obey the following constraints, Fig. 4(a):

$$K_D \geq K + \frac{\epsilon + l_{height}}{d} \tag{11}$$

$$l_{height} > \epsilon \tag{12}$$

$$r_0 > 2d + l_{robot}. \tag{13}$$

Condition (11) limits how far backward new depositions can extend into previously navigable terrain. It ensures that the motion and deposition strategy will not direct robots to deposit directly underneath themselves. Condition (12) ensures that the deposition mechanism has enough clearance to make depositions that conform with the assumptions in Alg.1. Condition (13), conservatively, ensures that a physical robot has enough space to back up.

The strategy in Alg. 2 is for a robot to move toward the goal location x_* unless it encounters a feature that impedes its progress, i.e. a point pair that violates the navigability condition (5). In that case, the robot deposits on the lower point and backs up to check that the new deposition does not in itself preset a non-navigable feature.

Theorem 7 *Given a robot that fulfills parameter conditions (11)-(13) with starting position x_0 that fulfills (10) following Alg. 2 will reach a goal point x_* after a finite number of steps.*

Proof. Denote the interval $[x_0 - r_0, x + d]$ in which no point pairs fulfill (8) by A (*accessible region*). Robots stay inside the accessible region at all times while finding points to deposit on. First, condition (12) guarantees a robot can make a deposition of height ϵ, as required by Alg. 1. Second, condition (11) guarantees that depositions with a maximum height of l_{height} made in the interval $[x, x + d]$ will not extend into $[x_0 - r_0, x - d]$. As a result, moving to $x - 2d$ after a deposition guarantees that no points in A fulfill (8). By (10) and the deposition strategy there are always accessible points, i.e. $[x_0 - r_0, x_0] \subset A$. By Alg. 1 this algorithm terminates after a finite number of depositions with $x = x_*$. $\square$

Figure 3 shows a series of depositions made via Alg. 2. This strategy also guarantees that robots can always reach x_0 without requiring additional depositions, which could allow robots to replenish supplies. Conversely, the accessible region provides cooperating robots access the deposition site, Sec. 4.2.

Physical depositions are not perfect cones, Fig. 1(b). Algorithm 2 explicitly allows for uncertainty in the target structure (via ϵ), but not for deposition uncertainty. In fact, the upper bound for target structures requires that no depositions accidentally make intermediate structures larger than $P_K[h_0]$. Following is a short description on how to address this problem and allow depositions with arbitrary continuous shape functions f (and bounded derivative f'_{max}), as long as f can be sandwiched between two cones, Fig. 4(b). As long as $l_{dep} < \epsilon$. Alg. 1 (and as a result Alg. 2) still work with the following substitutions: In Lem. 1 f'_{max} takes the place of K_D. In Thm. 4 the minimum height is $\epsilon - l_{dep}$ instead of ϵ. In Thm. 5 and condition (11)K_D is replaced with K_a. In addition to uncertainty in shape, this approach of bounding cones also allows for uncertainty in the exact deposition location and volume.

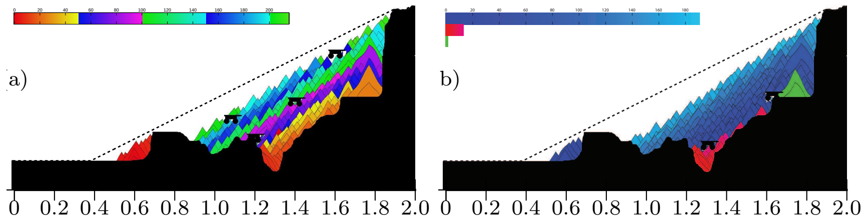

Fig. 5 Simulations of adaptive ramp building, in both simulations the parameters are $x_0 = 0.2$, $x_* = 1.9$, $d = 0.1$ and otherwise the same as in Fig. 3. (a) Example of cooperative, distribute ramp building. Each robot is limited to making 25 depositions each (indicated by a different continuous color gradient), after which time the active robot signals that it is out of material and a new robot begins. (b) Multiple robots all start simultaneously. If they become stuck, they stop moving and are treated as obstacles by other robots.

4.2 Adaptive Ramp Building with Multiple Robots

The locally reactive nature of Alg. 2 makes extension to multiple robots easy. For example, imagine that multiple robots—each with limited deposition capacity—cooperatively build a ramp. Robots avoid collisions and can communicate locally. One robot starts executing Alg. 2 while the others follow. Once a robot runs out of building material, it signals for another robot to execute Alg. 2, and returns to a base station at x_0, or it can simply stop and be treated as an obstacle by other robots, Fig. 5(a). This coordination strategy works due to the distributed nature of Alg. 2. Between robots, information about deposition locations is communicated through stigmergy.

Alternatively, multiple robots can start at different locations and execute Alg. 2 concurrently. For example, to build a large ramp toward a beacon multiple robots could be dropped along the construction path. Each robot starts building a ramp. However, without initially fulfilling starting condition (10) robots might become stuck, i.e. cannot move to an appropriate place to make a deposition, Fig. 5(b) right. Further, without coordination one robot might deposit on another, Fig. 5(b) middle. Despite these failures, if one robot initially fulfills (10) the process with successfully complete. Other robots can provide speed up through parallelism by partially building ramps until they become stuck.

4.3 Physical Implementation and Experimental Results

We built a remote controlled prototype robot, Fig. 1(b), and a scanning foam deposition mechanism, Fig. 6(a), for testing solutions to the key technical challenges presented by Alg. 2. The prototype shows that robots can, in principle, build and navigate relatively large foam structures. The scanning deposition mechanism demonstrates autonomous leveling behavior that can

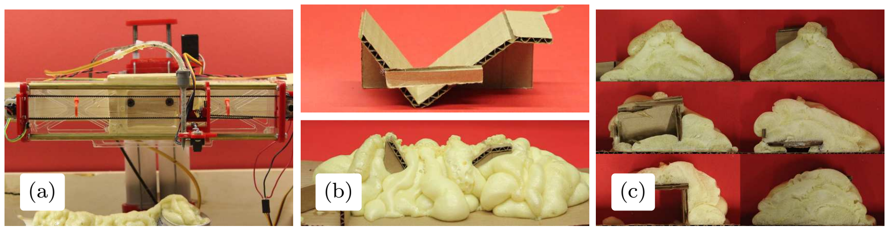

Fig. 6 Scanning foam deposition mechanism. (a) A scanning carriage holds a downward facing IR-distance sensor and mixing nozzle. Pressurized foam precursors are delivered to the nozzle by flexible tubing. (b) Top, Initial obstacle before leveling deposition. Bottom, final structure after deposition episode. (c) Cross sections of final structure. Each leveling deposition episode represents one cone-like deposition in Alg. 2.

be used to turn the physical three dimensional construction problem into the simplified two dimensional problem solved by Alg. 2.

One major challenge is designing a deposition mechanism and selecting an appropriate material [10]. The prototype robot and scanning deposition mechanism both use two compartment syringes with mixing nozzles (McMaster-Carr PN: 74695A11 with 74695A63, 7451A22 with 7816A32) and high expansion poly-urethane casting foam (US-Composites 2 lb foam) to make amorphous depositions.

The scanning deposition mechanism consists of a fixed structural frame and a moving carriage, Fig 6(a). By running a Alg. 1 along the direction of carriage travel (with $K = 0, \epsilon = 2\,\text{cm}$ and d equalling the entire range) this mechanism autonomously creates a level structure from amorphous depositions. Mounting this mechanism on the front of a robot and treating each leveling deposition episode as a single deposition in Alg. 2, turns the physical construction problem into the simplified model. Viewed from the side, each leveled line under the carriage represents the apex of a conical deposition. Algorithm 2 simply picks the next point to level.

5 Conclusion

We developed a continuous model for amorphous depositions, and used it to prove correctness of a distributed algorithm that solves the adaptive ramp building problem. This example application illustrates how locally reactive behavior and amorphous building material together can create reliable building behavior in unstructured terrain.

Adaptive ramp building can also serve as a base behavior for other, more complicated, behaviors. For example, it could be used to guarantee accessibility to locations where support structures need to be built. With the ability to consistently encode virtual points in a group of robots, adaptive ramp building could also be used directly to build arbitrary (K-Lipschitz) structures by building ramps to a carefully chosen set of virtual points: an approach we plan to explore in more detail.

There are a number of ways the presented algorithms could be improved. Our presentation focused on correctness, not optimality. Robots could be much smarter about picking deposition points and try to maximize the volume of each deposition, especially if their sensing radius was larger than d.

6 Proofs

Proof (Thm. 2). 2.1) Assume to the contrary that $\exists x, y \in Q$ s.t.

$$|P_K[h](x) - P[h](y)| > K|x - y|. \tag{14}$$

Assume w.l.o.g. that $P_K[h](y) \leq P_K[h](x)$ and since $P_K[h]$ is a positive scalar function $|P_K[h](x) - P[h]_K(y)| = P_K[h](x) - P_K[h](y)$. Rearranging the terms in (14) leads to the contradiction $P_K[h](x) - K|x - y| > P_K[h](y)$, since the max in $P_K[h](y)$, see (7), is taken over the entire domain, including x. Therefore points violating the Lipschitz condition cannot exist in $P[h]$. □

2.2) Assume to the contrary that there exists a point $x \in Q$ s.t. $P_K[h](x) > g(x) \geq h(x)$. Since there cannot be equality between $P_K[h](x)$ and $g(x)$ the maximization in (7) must take its maximum value at some other point $y \in Q$. Rearranging $P_K[h](x) = h(y) - k|x-y| > g(x)$ results in $h(y) - g(x) > k|x-y|$, and since $g > h$ $g(y) - g(x) > k|x - y|$ which is a contradiction, as it would violate the Lipschitz continuity of g. □

Proof (Thm. 5). First, note that P can be applied to non-continuous functions, specifically continuous structures with a single discontinuous point. Let $\widetilde{h}_{n,(\phi,\sigma)}(x) = h_n(x) + (\sigma - h_n(\phi))\delta_\phi x$ where δ denotes the Kronecker delta.

Next, since ϕ is in the search set of max for point $P_K[h_n](x)$ in (7) $h_n(\phi) \leq \sigma = h_n(\phi) + \omega \leq P_K[h_n](\phi)$, consequently

$$\widetilde{h}_{n,(\phi,\sigma)} \leq P_K[h_n]. \tag{15}$$

Finally, since restricting $y \in \{x, \phi\} \subset Q$ in (7) results in the same expression as (2) $D[f_{(\phi,\sigma)}, h_n] = h_{n+1} \leq P_{K_D}[\widetilde{h}_{n,(\phi,\sigma)}]$. Thus, $h_{n+1} \leq P_{K_D}[\widetilde{h}_{n,(\phi,\sigma)}]$.

By Thm. 3 and assuming that $K_D > K$, $P_{K_D}[\widetilde{h}_{n,(\phi,\sigma)}] \leq P_K[\widetilde{h}_{n,(\phi,\sigma)}]$. Together Thm. 2.2 and (15) imply that $P_K[\widetilde{h}_{n,(\phi,\sigma)}] \leq P_K[h_n]$, which results in the series of relations $h_{n+1} \leq P_K[\widetilde{h}_{n,(\phi,\sigma)}] \leq P_K \leq P_K[h_n]$. And again, by Thm. 2.2 $P_K[h_{n+1}] \leq P_K[h_n]$. However, $h_{n+1} \geq h_n$ implies $P_K[h_{n+1}] \geq P_K[h_n]$, thus $P_K[h_{n+1}] = P_K[h_n]$. By induction, $P_K[h_n] = P_K[h_0]$. □

References

1. S. Berman, A. Halasz, M. A. Hsieh, and V. Kumar. Optimized stochastic policies for task allocation in swarms of robots. *IEEE Transactions on Robotics*, 25(4):927–937, 2009.
2. T. Bonwetsch, F. Gramazio, and M. Kohler. Digitally fabricating non-standardised brick walls. In *ManuBuild*, pages 191–196, Rotterdam, Netherlands, 2007.
3. R. D'Andrea. Flying machine enabled construction: http://www.idsc.ethz.ch/Research_DAndrea/fmec, ongoing.
4. K. C. Galloway, R. Jois, and M. Yim. Factory floor: A robotically reconfigurable construction platform. In *IEEE International Conference on Robotics and Automation (ICRA)*, pages 2467–2472, may 2010.
5. D. Hjelle and H. Lipson. A robotically reconfigurable truss. In *Proceedings of ASME/IFToMM International Conference on Reconfigurable Mechanisms and Robots*, June 2009.
6. N. Khalili. *Emergency Sandbag Shelter: How to Build Your Own*. CalEarth Press, 2008.
7. B. Khoshnevis. Automated construction by contour crafting related robotics and information technologies. *Journal of Automation in Construction Special Issue: The best of ISARC 2002*, 13:5–19, 2004.
8. D. Ladley and S. Bullock. Logistic constraints on 3d termite construction. In *Fourth International Workshop on Ant Colony Optimization and Swarm Intelligence*, pages 178–189, 2004.
9. Q. Lindsey, D. Mellinger, and V. Kumar. Construction of cubic structures with quadrotor teams. In *Proceedings of Robotics: Science and Systems*, Los Angeles, CA, USA, June 2011.
10. N. Napp and E. Klavins. A compositional framework for programming stochastically interacting robots. *The International Journal of Robotics Research*, 30(6):713–729, 2011.
11. N. Napp, O. Rappoli, J. Wu, and R. Nagpal. Materials and mechanisms for amorphous robotic construction. In *Proceedings of IEEE/RSJ International Conference on Intelligent Robots and Systems (IROS)*, 2012.
12. A. W. Naylor and G. R. Sell. *Linear Opearator Theory in Engineering and Science*. Applied Mathematical Sicences. Springer, 1982.
13. K. Petersen, R. Nagpal, and J. Werfel. Termes: An autonomous robotic system for three-dimensional collective construction. In *Proceedings of Robotics: Science and Systems*, Los Angeles, CA, USA, June 2011.
14. S. Revzen, M. Bhoite, A. Macasieb, and M. Yim. Structure synthesis on-the-fly in a modular robot. In *Proceedings of IEEE/RSJ Conference on Intelligent Robots and Systems (IROS)*, 2011.
15. G. Theraulaz and E. Bonabeau. Coordination in distributed building. *Science*, 269, 1995.
16. J. S. Turner. *The Externded Organism. The Physiology of Animal-Built Structures*. Harvard University Press, 2004.
17. Northwestern Division US Army Corps of Engineers. *Sandbagging Techniques*, 2004.
18. J. Werfel and R. Nagpal. Three-dimensional construction with mobile robots and modular blocks. *Int. J. Rob. Res.*, 27:463–479, March 2008.